



# Hybrid $\text{CF}_x\text{-Ag}_2\text{V}_4\text{O}_{11}$ as a high-energy, power density cathode for application in an underwater acoustic microtransmitter

Praveen Meduri, Honghao Chen, Xilin Chen, Jie Xiao, Mark E. Gross, Thomas J. Carlson, Ji-Guang Zhang, Z. Daniel Deng\*

Pacific Northwest National Laboratory, Richland, WA 99354, United States

## ARTICLE INFO

### Article history:

Received 8 July 2011

Received in revised form 2 August 2011

Accepted 2 August 2011

Available online 10 August 2011

### Keywords:

Carbon fluoride

Silver vanadium oxide

High power density

Cathode

Primary lithium battery

Micro battery

## ABSTRACT

This study demonstrates the excellent electrochemical performance of the hybrid carbon fluoride ( $\text{CF}_x$ )/silver vanadium oxide (SVO)/graphene(G) cathode and its potential utilization in the Juvenile Salmon Acoustic Telemetry System (JSATS). The impedance increase caused by LiF formation is effectively addressed by silver metal deposition during SVO reduction. The coexistence of graphene additive reduces the initial voltage delay; thus, a prolonged operation voltage is observed with enhanced electronic conductivity, with specific capacity of  $\sim 462 \text{ mAhg}^{-1}$  at 5C rate and  $661 \text{ mAhg}^{-1}$  at 1C rate. The peak current delivered from the as-designed hybrid cathode is improved over the commercial Zn/ $\text{Ag}_2\text{O}$  batteries, suggesting battery size/weight reduction critical for the JSATS transmitters.

© 2011 Elsevier B.V. All rights reserved.

## 1. Introduction

Primary batteries are of great interest as portable energy storage devices in electronics, medical implants, army applications, and acoustic telemetry. The Juvenile Salmon Acoustic Telemetry System (JSATS) is a nonproprietary sensing technology for monitoring the behavior and survival of juvenile salmon passing through hydroelectric facilities [1–3]. The current JSATS transmitter weighs 430 mg and uses two size-337 watch batteries stacked in series to produce 3 V output; each battery weighing 130 mg. Therefore, reduction in size and weight of the batteries is critical. Among different cathodes for primary lithium batteries,  $\text{CF}_x$  ( $0 < x < 1$ ) has the highest theoretical specific capacity of  $864 \text{ mAhg}^{-1}$  for a fluorine content of one [4] while the theoretical capacity of Zn– $\text{Ag}_2\text{O}$  battery is  $180 \text{ mAhg}^{-1}$ . Hence, the operational voltage and the gravimetric density can be significantly improved compared with Zn– $\text{Ag}_2\text{O}$  couple. The capacity, however, varies with the fluorine content.  $\text{CF}_x$  is intrinsically not a good electronic conductor, which leads to initial voltage delay and low rate capability, inhibiting its application in high-power devices. In a typical Li/ $\text{CF}_x$  cell, the cell impedance mainly comes from the cathode in which LiF continues to form during discharge. Numerous efforts broadly classified into two categories have focused on addressing these problems, but rate capability is still a concern. The first approach is to make  $\text{CF}_x$  conductive by decreasing the fluorine content to form

sub-fluorinated carbons ( $\text{CF}_x$ ;  $x < 1$ ) [5,6] or by thermal/chemical treatment [7–10].  $\text{CF}_x$  with varied fluorine content has been studied to show capacities of  $\sim 400 \text{ mAhg}^{-1}$  at rates as high as 2.5C [4] but is built on capacity sacrifice due to the reduced amount of fluorine in  $\text{CF}_x$ . The second approach is to mix the  $\text{CF}_x$ -based materials with other cathode materials such as  $\text{MnO}_2$  [11], SVO [12–14] and  $\text{MoO}_3$  [15] to develop a hybrid structure, but the progress in this area is limited without significant improvement on the rate performance.

This study presents a simple and scalable approach to prepare CF/SVO hybrid cathodes with tunable energy/power densities to satisfy different wireless energy requirements. In particular, the addition of only 3% graphene to CF/SVO hybrid material delivers  $462 \text{ mAhg}^{-1}$  capacity at 5C, which is the highest reported until now in CF-based material systems. The potential application of the as-designed hybrid cathode also is demonstrated here by incorporating the micro battery in a transmitter to track juvenile salmon.

## 2. Experimental methods

Carbon monofluoride (CF), carbon-coated carbon monofluoride (CCF) (Advanced Research Chemicals, Inc.), and SVO (Inframat Advanced Materials) were used as-received without further treatment. To synthesize the hybrid materials, CF and SVO were mixed in the weight ratio of 80:20. In the samples with carbon, 3% Super P carbon (Timcal) or graphene was added to the mixture, which contains 80:17 of CF and SVO, respectively. All the samples were ball-milled in a SPEX P sample preparation 8000 M mixer/mill for 1 h in intervals of 15 min, with 15 min of rest between each interval.

\* Corresponding author. Tel.: +1 509 372 6120; fax: +1 509 372 6089.  
E-mail address: [Zhiqun.deng@pnnl.gov](mailto:Zhiqun.deng@pnnl.gov) (Z.D. Deng).

The slurry consisted of 85 wt.% active material, 10 wt.% Super P carbon, and 5 wt.% of PVDF as the binder dissolved in 1-methyl-2-pyrrolidinone (Sigma Aldrich) solvent. The slurry was mixed overnight using a magnetic stirrer at 750 rpm. The mixture was cast onto aluminum foil using a 7–8 mil thickness coater for all the samples on a Hohsen Corporation mini-coater (model MC10) with a mass loading in the range of 1–1.5 mg cm<sup>-2</sup>. The cast film after drying was punched into required sizes and then vacuum-dried overnight at 70 °C. A two-electrode coin cell was assembled using lithium as the counter electrode and 1 M LiPF<sub>6</sub> in EC: DMC (1:1 ratio by volume) as the electrolyte. An Arbin tester (model BT-2000) was used for the charge/discharge characteristics. CH Instruments potentiostat/galvanostats (models 6005D and 604D) were used for the impedance analysis and transmitter peak characteristics. The impedance was performed over a frequency range of 100 kHz to 5 MHz with amplitude of 10 mV.

### 3. Results and discussion

CCF exhibits capacities of 500 and 183 mAhg<sup>-1</sup> at 1C and 2C rates, respectively (Fig. 1a). The improved rate performance of the CF and SVO hybrid material is presented in Fig. 1b with capacities of 635 and 346 mAhg<sup>-1</sup> at rates of 1C and 2C, respectively. However, the voltage is significantly lower for the 2C rate, with high initial voltage delay. The voltage delay is reduced and the rate characteristics are improved with the addition of 3% SP carbon (Fig. 1c). The best performance, however, is obtained by replacing the SP carbon with the same amount of graphene (Fig. 1d). A specific capacity of 663 mAhg<sup>-1</sup> is obtained per wt. of composite material which corresponds to

776 mAhg<sup>-1</sup> per wt. of CF at a C/10 rate. The theoretical capacity of the composite material is ~744 mAhg<sup>-1</sup> based on 80 wt.% CF<sub>x</sub> and 20 wt.% SVO. At a low rate, the lower capacity when compared to the theoretical capacity can be attributed to the partial decomposition of CF<sub>x</sub> during the high energy ball milling process. Particularly, the material shows capacities of 656 and 661 mAhg<sup>-1</sup> at rates of C/5 and 1C which correspond to 777 and 800 mAhg<sup>-1</sup> per unit weight of CF. At similar rates, CCF shows much lower capacities. The polarization is minute when the current rate is increased from C/10 to C/5 (Fig. 1d). However, the polarization increases with increasing discharge rates, which can be attributed to the difference in the potential of the solvated lithium ion [16,17]. As the bonding between the solvent and Li<sup>+</sup> ions increases, the difficulty to form a Li–F pair increases, leading to an increase in the F ion activity, reducing the reaction potential leading to the large polarization that we see with increasing discharge rates. The hybrid material with graphene does not show a significant voltage delay except at a 5C rate, and retains capacities of 588 and 462 mAhg<sup>-1</sup> at 2C and 5C rates, respectively.

To further emphasize our findings, an impedance analysis at 10% depth of discharge state was performed. The Nyquist plots for impedance are shown in Fig. 2a, and the equivalent circuit in Fig. 2b. The bulk resistance arising from the electrodes, electrolyte, and the current collectors is low for all the materials. On the interface between the liquid electrolyte and the discharge product shell, the charge transfer through an existing electric double layer can be characterized by  $Q_{ct}$  and  $R_{ct}$  at high frequency. The discharge product shell on the active material can be characterized by  $Q_1$  (a constant phase element) and  $R_1$  (resistance to lithium ion diffusion in the discharge product shell) at high frequency.

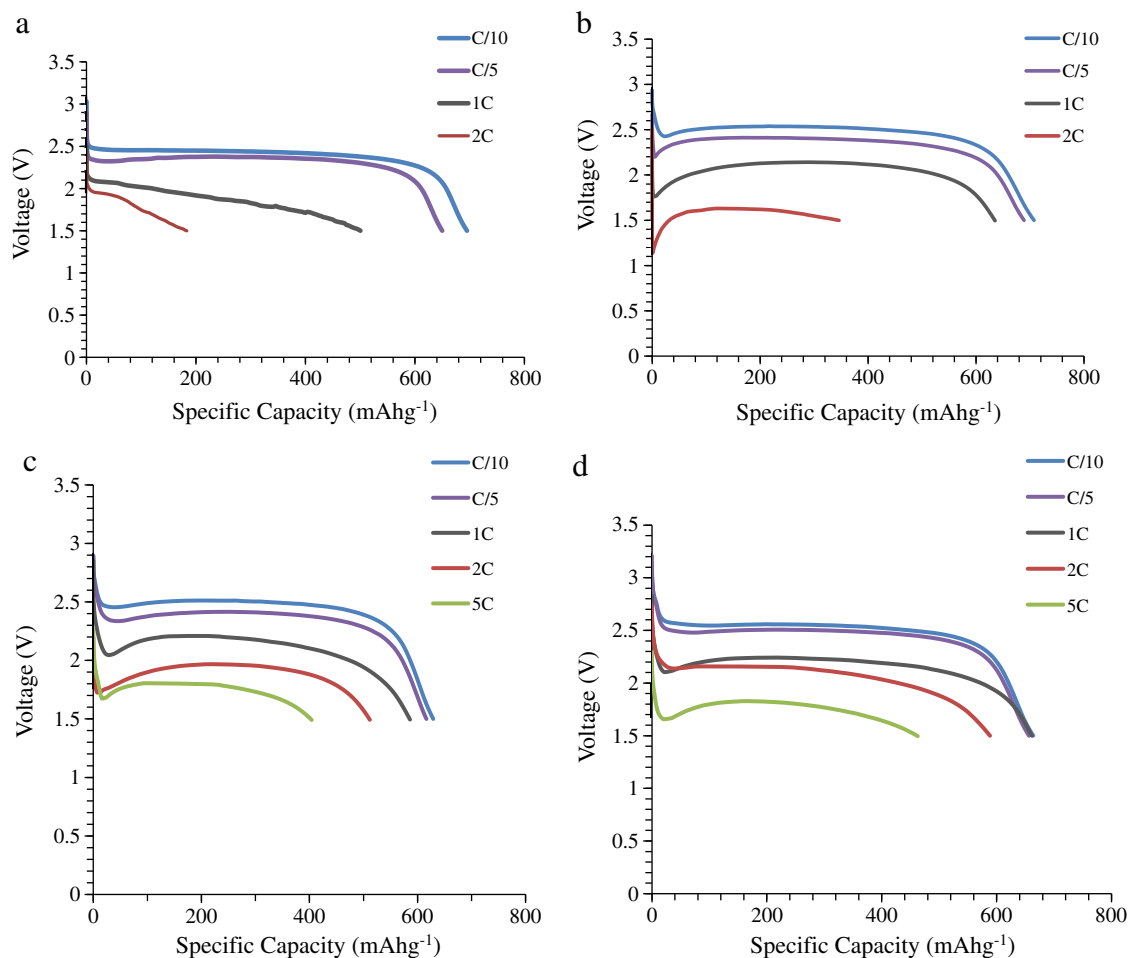
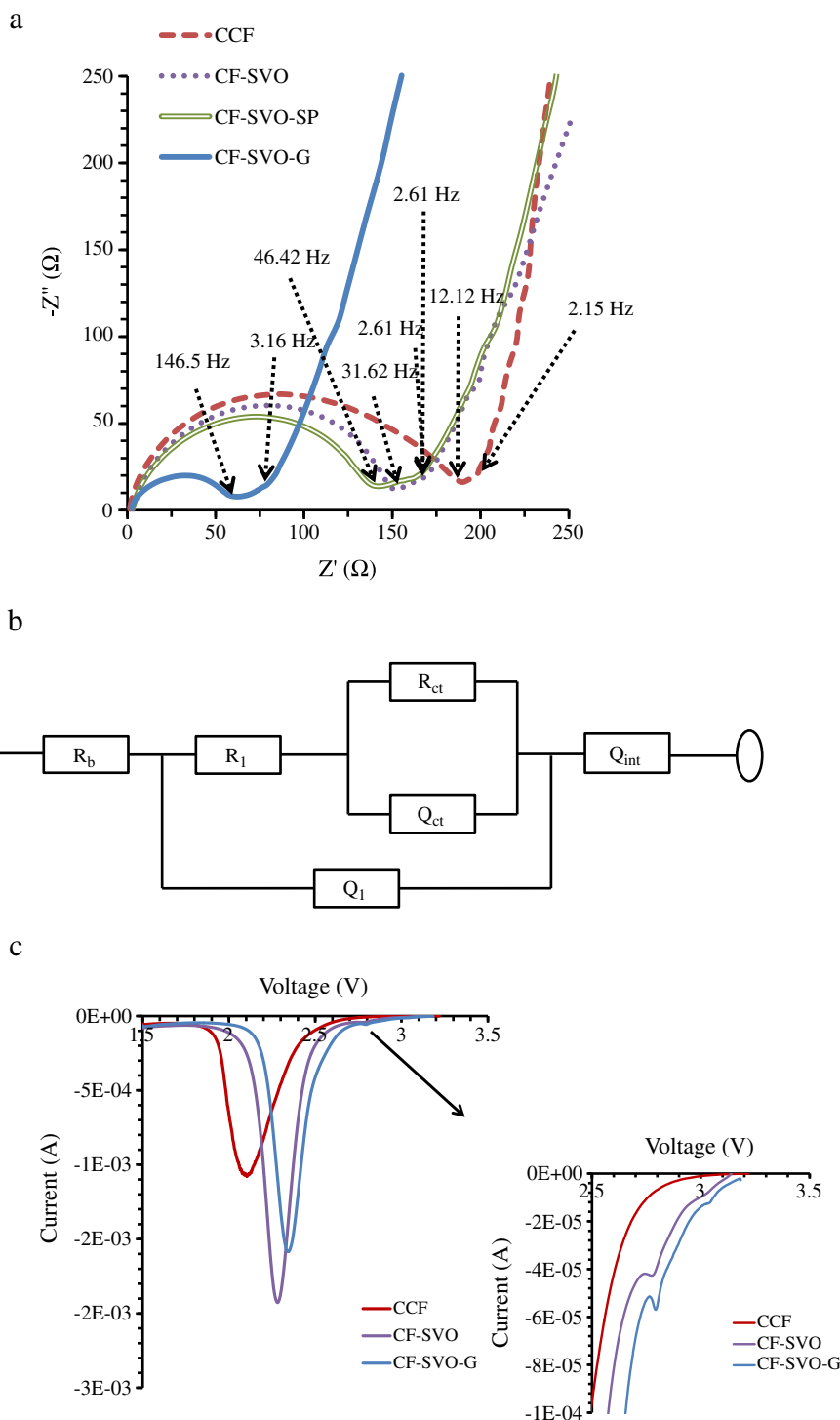


Fig. 1. Discharge profiles at different current densities of (a) carbon-coated carbon fluoride (CCF), (b) ball-milled CF-SVO hybrid, (c) ball-milled CF-SVO-SP carbon hybrid, (d) ball-milled CF-SVO-graphene hybrid.



**Fig. 2.** (a) Impedance spectra for different hybrid materials and CCF at 10% DoD. (b) Complete cell equivalent circuit for the composite materials and CCF. (c) Linear scan voltammetry curves with marked silver reduction peaks in the inset.

After diffusing through the product shell, lithium ion reacts with  $\text{CF}_x$  readily at the interface. Due to the lack of lithium ion diffusion in the active materials, this process is best represented by a constant phase element  $Q_{\text{int}}$ . A similar equivalent circuit for graphite electrode by M.D Levi and D. Aurbach [18] supports our explanation. The total cell resistance follows the order of  $\text{CCF} > \text{CF/SVO} > \text{CF/SVO/SP} > \text{CF/SVO/G}$ , indicating that hybrid material with graphene has significantly low resistance with improved conductivity. The onset between the semicircle and the sloped line are indicative of reaction kinetics with

higher frequencies representing faster reaction kinetics, which indicates primarily low reaction resistance [10]. The frequencies between the onsets clearly marked in Fig. 2a indicate that the reaction kinetics of CF/SVO/G is the fastest and that of CCF are the slowest; the reaction kinetics of the other materials falls between these two which suggests that graphene obviously plays a key role. Compared with Super P, graphene nanosheets form a better continuous conductive network which not only anchor the  $\text{CF}_x$  particles but also provide an ideal substrate for Ag deposition during discharge. The conductivity

improvement through Ag formation is therefore more effective in graphene than that of Super P in which isolated carbon particles are unavoidable. Linear scanning voltammetry curves for CCF, CF-SVO, and CF-SVO-G (Fig. 2c) indicate higher reduction potentials for the hybrid materials compared to CCF, which is clearly evident in the rate

dependence discharge study. The inset of Fig. 2c indicates a peak at 2.8 V corresponding to the reduction of silver in SVO for both hybrid materials [19].

A Ragone plot in Fig. 3a indicates that the energy density and power density of the CF/SVO/G composite is significantly higher than that of other materials. The drastic difference in the power density of the material can be attributed to the two factors mentioned above: (1) CF inherently consists of CF<sub>2</sub> and CF<sub>3</sub> surface groups, which gives rise to the high intrinsic resistivity. However, ball milling with carbon leads to removal of these resistive surface groups and homogeneously distributes carbon forming a continuous network, significantly improving the conductivity and hence, low voltage delay. Especially, if SP is added during the electrode slurry mixing step the conductive network formed always contains isolated carbon particles which do not help the high rate performance. (2) Ag formed exists between the interface of SVO and the carbon additives since only those SVO particles that have good contact with carbon can accept electrons to reduce Ag. It is the deposition of Ag<sup>+</sup> within the carbon network that further interconnects the CF<sub>x</sub> domains and improves the electrode conductivity. At low rates, all materials show similar capacities, whereas CF/SVO/carbon composites show a steady performance with the increasing C rates until 5C (Fig. 3b). However, capacity per unit weight of CF material reveals significant improvement for CF/SVO hybrid materials, even at low rates. CF/SVO/G coin cells were used to measure the transmitter characteristics consisting of an ASIC circuit with a signal pulse every 3 seconds (Fig. 3c). Hybrid material shows a peak current (~2.7 mA) stronger than the watch battery currently used for the transmitter (~2.4 mA), indicating the potential practical applicability in transmitters. Further material investigation is being conducted to optimize the composite material for required performance with greatly reduced battery weight and volume.

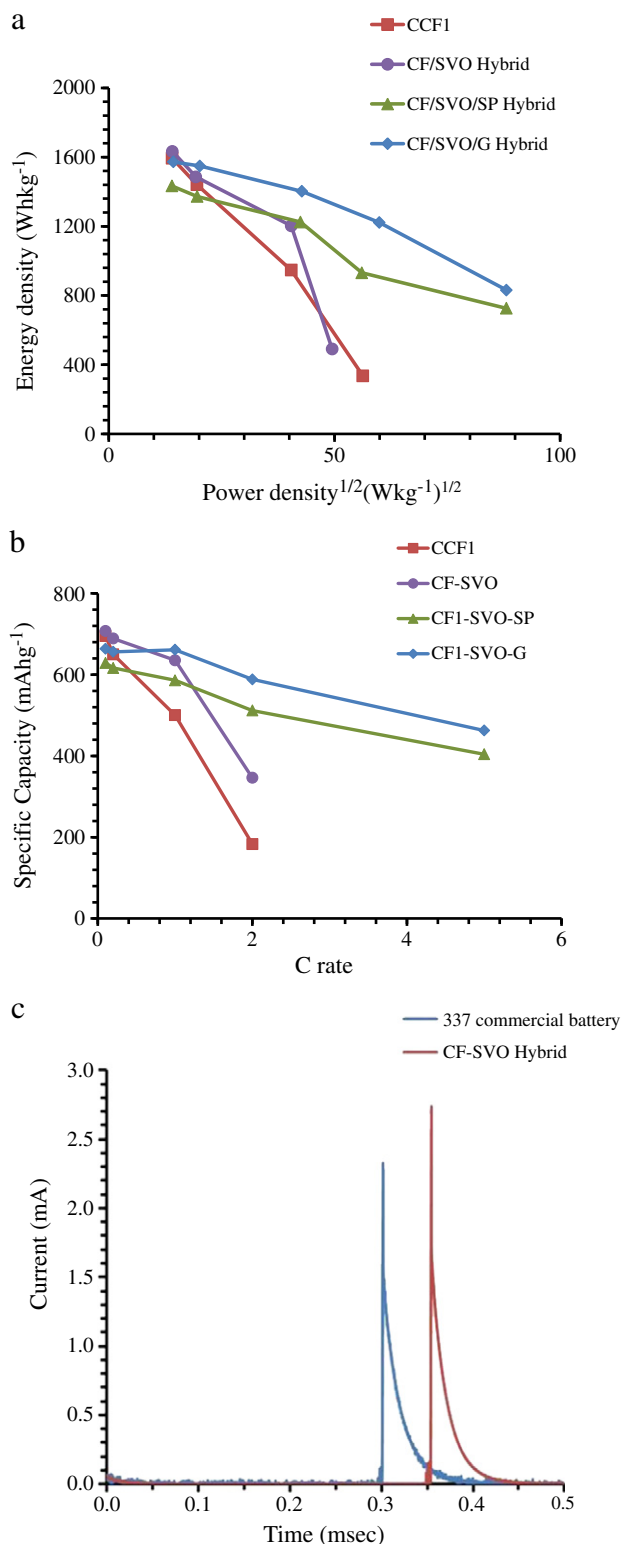


Fig. 3. (a) Ragone plot of the different Li/hybrid cells and Li/CCF cells. (b) Rate performance of the hybrid materials and CCF. (c) Transmitter peak current characteristics.

#### 4. Conclusions

CF/SVO hybrid materials have been developed by high-energy ball milling process for the first time. The as-synthesized hybrid material with 3% graphene exhibits capacity of 776 mAhg<sup>-1</sup> per unit weight of CF and ~462 mAhg<sup>-1</sup> at current density of 5C. The impedance analysis shows that the charge transfer resistance for the CF/SVO/G hybrid is the lowest, accounting for excellent rate capability and low initial voltage delay. In particular, Ag formed during SVO reduction in conjunction with carbon helps in attaining higher discharge profiles and enhanced conductive properties between CF domains and the current collector, creating multiple electron pathways leading to improved rate performance.

#### Acknowledgements

The study was funded by the U.S. Army Corps of Engineers (USACE), Portland District. Brad Eppard is the technical lead for USACE and we greatly appreciate his involvement and oversight.

#### References

- G.A. McMichael, M.B. Eppard, T.J. Carlson, J.A. Carter, B.D. Ebberts, R.S. Brown, M.A. Weiland, G.R. Ploskey, R.A. Harnish, Z.D. Deng, *Fisheries* 35 (2010) 9.
- M.A. Weiland, Z.D. Deng, T.A. Seim, B.L. Lamarche, E.Y. Choi, T. Fu, T.J. Carlson, A.I. Thronas, M.B. Eppard, *Sensors* 11 (2011) 5645.
- Z.D. Deng, M.A. Weiland, T. Fu, T.A. Seim, B.L. Lamarche, E.Y. Choi, T.J. Carlson, M.B. Eppard, *Sensors* 11 (2011) 5661.
- P. Lam, R. Yazami, J. Power Sources 153 (2006) 354.
- R. Yazami, A. Hamwi, K. Guérin, Y. Ozawa, M. Dubois, J. Giraudet, F. Masin, *Electrochem. Commun.* 9 (2007) 1850.
- K. Guérin, R. Yazami, A. Hamwi, *Electrochem. Solid-State Lett.* 7 (2004) A159.
- S.S. Zhang, D. Foster, J. Read, *J. Power Sources* 188 (2009) 601.
- Y. Li, Y. Chen, W. Feng, F. Ding, X. Liu, *J. Power Sources* 196 (2011) 2246.
- Q. Zhang, S. D'Astorg, P. Xiao, X. Zhang, L. Lu, *J. Power Sources* 195 (2010) 2914.
- S.S. Zhang, D. Foster, J. Read, *J. Power Sources* 191 (2009) 648.
- A. Kozawa, *J. Electrochem. Soc.* 134 (1987) 780.
- H. Gan, R.S. Rubino, E.S. Takeuchi, *J. Power Sources* 146 (2005) 101.

- [13] K. Chen, D.R. Merritt, W.G. Howard, C.L. Schmidt, P.M. Skarstad, J. Power Sources 162 (2006) 837.
- [14] P.M. Gomadam, D.R. Merritt, E.R. Scott, C.L. Schmidt, P.M. Skarstad, J.W. Weidner, J. Power Sources 174 (2007) 872.
- [15] S.J. Ebel, S.A. Smesko, E.S. Takeuchi, , 1997 (U. S. Patent 5,667,916).
- [16] S.S. Zhang, D. Foster, J. Wolfenstine, J. Read, J. Power Sources 187 (2009) 233.
- [17] N. Watanabe, R. Hagiwara, T. Nakajima, H. Touhara, K. Ueno, *Electrochim. Acta* 27 (1982) 1615.
- [18] M.D. Levi, D. Aurbach, J. Phys. Chem. B 101 (1997) 4630.
- [19] E.S. Takeuchi, W.C. Thiebolt III, J. Electrochem. Soc. 135 (1988) 2691.